

Prostate IMRT fractionation strategies: two-phase treatment versus simultaneous integrated boost

Pavel Stavrev and Dimitre Hristov

Medical Physics Unit, Montreal General Hospital & McGill University, 1650 Cedar Ave.,
Montreal, H3G 1A4, Canada

Background. The purpose of the study was to investigate the radiobiological effect of the number of fractions, position uncertainties and clonogen spread (microscopic disease) on two different inverse treatment planning alternatives: (a) 2-phase strategy; (b) simultaneous integrated boost (SIB).

Material and methods. The tumour control probability (TCP) and normal tissue complication probability (NTCP) were calculated for the 2-phase strategy, which has well defined fractionation scheme and compared to the TCP and NTCP for the SIB strategy calculated as a function of the number of fractions. For a 7-beam IMRT prostate treatment, we have performed inverse treatment planning for the two different strategies following the above method.

Results. When the position uncertainties and clonogen spread were accounted for in the TCP calculation a drop as large as 10% was found. A drop of 5-7% in the TCP was obtained for the SIB strategy, if delivered in the same number of fractions as the 2-phased one.

Conclusions. The potential of inverse planning to design tight conformal dose distributions is fully revealed in the SIB optimization process. The optimized SIB superior dose distributions require modification of the delivered dose per fraction and therefore careful selection of the fractionation regime. Hence physically optimized SIB treatments may not always lead to better tumour control and tissue sparing.

Key words: prostatic neoplasms - radiotherapy; radiotherapy, conformal; radiotherapy dosage; dose fractionation

Introduction

The availability of inverse planning and intensity modulated radiotherapy (IMRT) technology opened the possibility of designing new treatment strategies with superior dose distributions, namely tighter treatment margins and therefore better organ sparing.

Recently Mohan et al.,¹ and Wu et al.,² have suggested a »simultaneous integrated boost« (SIB) IMRT approach to head and neck

Received 1 April 2003

Accepted 6 May 2003

Correspondence to: Pavel Stavrev, Ph.D., (currently at) Department of Medical Physics, Cross Cancer Institute, 11560 University Ave, Edmonton, Alberta, T6G 1Z2, Canada; E-mail: pstavrev@phys.ualberta.ca

This work is supported by an MRC grant MOP 36470.

cancer, leading to better conformity and superior dose distributions in the organs at risk compared to a standard way of radiation treatment planning. The SIB strategy was proposed as an alternative to the commonly used two-phase radiation therapy. The idea itself, namely, - uniting the conventional 2-phase treatment strategy in one, is not new, it was considered by a number of authors before.³⁻⁶ The application of IMRT to it is the important new development. In their study this approach was applied to head and neck cancer. In this paper we consider the SIB approach applied to the case of prostate cancer taking the effect of position uncertainties and possible clonogen spread into account. Further development of the investigations of Mohan et al.,¹ is conducted by more detailed radiobiological analyses. While, the main quantity under consideration in Wu et al.² was the »normalized total dose« NTD (similarly to Lebesque and Keus),³ here we demonstrate the application of tumour control probability (TCP) and normal tissues complication probability (NTCP) models to evaluate the SIB IMRT plans as a function of the number of fractions. We demonstrate with this work that the SIB IMRT physical optimization, although leading to superior dose distributions in physical terms - with respect to specified dose and dose-volume criteria - may result in lower tumour control or higher probability for organ damage depending on the fractionation strategy chosen.

Material and methods

Treatment strategies

A patient who had recently undergone radiation treatment for the carcinoma of the prostate in our centre was re-planned with inverse planning for the purpose of this study (Figures 1a, b, c). The original treatment technique employed a four-field box arrangement (Plan I) with 18 MV MLC-shaped conformal beams to deliver a uniform dose of 44 Gy to planning target volume I (PTV1) in 22 daily fractions. In the second phase of the treatment (Plan II), a three-field technique with one anterior (gantry angle 0°) and two posterior lateral fields (gantry angles 260° and 100°) was employed to deliver a boost of 26 Gy to planning target volume II (PTV2) in 13 daily fractions. PTV1 encompassed the gross tumour volume (GTV) with a uniform 1.5 cm margin to account for microscopic disease, set-up uncertainties, and organ motion. PTV2 encompassed the GTV with a uniform 0.5 cm margin to account for set-up uncertainties and organ motion. In both phases the patient was treated in supine position.

A 7-beam treatment technique (Figures 1b, 1c) was optimized with the Helios inverse planning option of the CadPlan treatment planning system (Varian Medical Systems, Palo Alto, CA). For the two-phase strategy, Plan I and Plan II were optimized separately with the optimization parameters listed in Table 1. In terms of target coverage and bladder/rectum sparing these parameters resulted in dose distributions superior to the ones delivered by the original forward treatment

Table 1. Inverse treatment planning dose and priority prescriptions for the different treatment strategies

	PTV1			PTV2			Bladder		Rectum	
	D _{min} [Gy]	D _{max} [Gy]	Priority	D _{min} [Gy]	D _{max} [Gy]	Priority	D _{max} [Gy]	Priority	D _{max} [Gy]	Priority
Plan I	44	44	100 %				33.9	50 %	26.4	50 %
Plan II				26	26	100 %	20.0	50 %	15.6	50 %
SIB44	44	70	100 %	70	70	100 %	53.9	50 %	42.0	50 %
SIB55	55	70	100 %	70	70	100 %	53.9	50 %	42.0	50 %

technique. Note that, in relative terms, the dose and the priority prescriptions for Plan I and Plan II in Table 1 are identical.

For the single phase, simultaneous integrated boost (SIB) strategy, both PTV1 and PTV2 were included in the optimization process and the prescription dose levels were combined to reflect the goal of the treatment in terms of total doses. Thus the SIB optimization prescribes 70 Gy to PTV2 and given the initial PTV1 objective of the 2-phase strategy - a minimum of 44 Gy to PTV1 (Table 1). However, after adding the two dose distributions optimized separately in the two-phase strategy, the minimal dose to PTV1 was found to be 55 Gy. Thus, two SIB plans with different minimum dose prescriptions to PTV1 were optimized (Table 1). Hereafter these are referred to as SIB44 and SIB55.

Biological models

In order to estimate the biological effect of a given dose distribution to the tumour or the organs at risk, the biologically equivalent dose was calculated. Based on it the TCP and NTCP were calculated using the model functions and the parameter estimates by.⁷⁻¹⁰

BED calculation

For each point (voxel) *ijk* from a certain structure the BED was calculated as:

$$[1] \text{BED}_{ijk} = D_{ijk} \left(1 + \frac{\beta d_{ijk}}{\alpha} \right); \quad d_{ijk} = \frac{D_{ijk}}{n_{fr}}$$

where α/β ratios of 10, 6 and 3.9 for the tumour, bladder and rectum respectively,¹¹ were used. Following the recent suggestions of Brenner et al.^{12,13} initiating the discussion¹⁴⁻¹⁷ about the possible low α/β ratio for prostate, we have investigated the case of tumour α/β of 2 Gy as well.

For the two-phased approach the BED is the sum of:

$$[2] \text{BED}_{ijk} = D_{ijk}^{PTV1} \left(1 + \frac{\beta d_{ijk}^{PTV1}}{\alpha} \right) + D_{ijk}^{PTV2} \left(1 + \frac{\beta d_{ijk}^{PTV2}}{\alpha} \right); \quad d_{ijk}^{PTV1} = \frac{D_{ijk}^{PTV1}}{m_p}; \quad d_{ijk}^{PTV2} = \frac{D_{ijk}^{PTV2}}{k_p}$$

where the index PTV1 refers to the dose distribution for the treatment of the larger volume accounting for the clonogen spreads, PTV2 refers to the boost volume and m_p and k_p are the number of fractions for both consecutive phases.

Because of the higher dose uniformity in the tumour, Eq. [2] is identical to Eq. [1]: $n_{fr} = m_p + k_p$; $D_{ijk} = D_{ijk}^{PTV1} + D_{ijk}^{PTV2}$. However, this statement does not hold true when the normal tissue is considered due to the significant dose heterogeneity throughout volumes of normal tissues in the vicinity of the treated targets. In this case each normal tissue voxel has different dose per fraction, which changes from phase-1 to phase-2.

It should be noted here that for the purposes of the biological index estimation in the 2-phase strategy, the DVHs are rather useless tool. This is why the TCP/NTCP estimation was done on the bases of the BED distributions instead of BED DVHs. Some authors^{11,18} use NTD - the dose corresponding to a standard $d_f = 2$ Gy dose per fraction regime:

$$[3] D'_{ijk} = D_{ijk} \left[\left(\frac{\alpha}{\beta} + d_{ijk} \right) / \left(\frac{\alpha}{\beta} + d_{std} \right) \right]$$

instead BED, for the NTCP calculations.

TCP and NTCP estimation

The TCP is calculated by the following formula:

$$[4] \text{TCP} = 0.5 \frac{1}{N} \sum \exp \left[\frac{2\gamma_{50}}{\ln 2} \left(1 - \frac{D_{ijk}}{D_{50}} \right) \right]$$

The values of the parameters for prostate tumours (T3 stage) are: $\gamma_{50}=0.95$, $D_{50}=46.3$, as estimated in the work of Okunieff et al.⁹

There are several models for NTCP estimation. Here, the Lyman phenomenological model¹⁹ and the Critical Volume (CV) population model^{10,20-25} are used. The Lyman phenomenological model is given by:

$$[5] \text{NTCP} = \Phi \left(\frac{D_{eff} - D_{50}}{\sigma_{D_{50}}} \right) = \Phi \left(\frac{D_{eff} - D_{50}}{m D_{50}} \right)$$

where, the effective dose corresponding to a given dose distribution is,

$$[6] D_{eff} = \left(\frac{1}{N} \sum \sqrt[n]{D_{ijk}} \right)^n$$

This formula was first derived in an explicit form by Niemierko and Goitein²⁶ and reflects a histogram reduction algorithm proposed by Lyman and Wolbarst.²⁷ It was shown by Niemierko and Goitein²⁶ that this reduction scheme is consistent with the Critical Element model. It was also shown by Niemierko and Goitein²⁶, that the Kutcher and Burman reduction algorithm^{28,29} is closely related to the Lyman and Wolbarst²⁷ one. Formula [5] was recently proposed by Niemierko³⁰ as a generalization of the equivalent uniform dose notion.

In the above formulae D_{ijk} denotes the dose to the ijk -th voxel, N is the total number of voxels in a structure. The values of the NTCP parameters are $n=.5; m=.11; D_{50}=80$ Gy (bladder) and $n=.12; m=.15; D_{50}=80$ Gy (rectum).⁸ Recently, several authors have considered the dose delivered to the rectal wall only,^{18,31-34} as a complication factor, introducing the usage of dose wall or dose surface histograms (DWH and DSH). In those works no parameter estimates are given and as far as the Burman et al.⁸ parameter values were calculated having in mind the dose to the whole volume, rather than the wall volume, here the NTCP are estimated based on the whole rectal and bladder volumes. Interestingly enough,^{18,31} report negligible differences in the NTCPs estimated by Lymans model and Burman et al.⁸ parameters based on the wall and whole rectal volume. Same results, for rectum, are obtained by Ting et al.³² using the critical element model.²⁶

On the other hand we consider incorrect the application of the parameters given by Burman et al.⁸ for estimations using the DWHs because those parameters have been obtained by fits to a »data set« that did not

have such sophisticated tools to extract rectum dose wall distributions.⁷

It should be emphasized that among the parameters estimated by Burman et al.⁸ there are some sets, which are considerably unreliable, like those for rectum. If one examines closely the dose-volume effects reported in the »Emami data«³⁵ it becomes obvious that in this case there are only 2 points for rectum and determining 3 parameter values from 2 data points is quite a long shot! Nevertheless these parameter values are used by many authors^{11,18,31-33} and are found to produce reasonable NTCP values.

For a comparison, we have also estimated the NTCP for bladder using the critical volume (CV) population model^{10,25} given with the following formulae:

$$[7] NTCP = \Phi \left(\frac{-\ln(-\ln \bar{\mu}_d(\gamma_{50}^{FSU}, D_{50}^{FSU}, D_{ijk})) + \ln(-\ln \mu_{cr})}{\sigma_{-\ln(-\ln \mu_{cr})}} \right)$$

$$[8] \mu_d = \frac{1}{N} \sum \Phi \left(\sqrt{2\pi} \gamma_{50}^{FSU} \ln \frac{D_{ijk}}{D_{50}^{FSU}} \right)$$

The parameters for bladder, estimated based on the »Emami data«,³⁵ are taken from Stavrev et al.¹⁰ and are $\mu_{cr} = 0.26 \pm 0.11$, $\sigma_{\mu_{cr}} = 0.07 \pm 0.03$, $D_{50}^{FSU} = 108 \pm 24$ [Gy], $\gamma_{50}^{FSU} = 0.8 \pm 0.2$. However, Stavrev et al.¹⁰ didn't bring out the parameter estimates for rectum due to the lack of data for their determination. A claim for CV model parameter estimation for rectum is made in the work of Hartford et al.,³⁶ based on 41 patients. Unfortunately, the parameter values are not given in this work.

In the above-presented TCP and NTCP estimation models, the response of the tissues to the variable fraction size is accounted for by a substitution of the voxel doses D_{ijk} by the biologically equivalent voxel doses BED_{ijk} .

Accounting for the position uncertainties and clonogen spread

One of the reasons behind the two phase strategy is that the slightly enlarged (in respect to GTV) volume (PTV2) is to account for

the position uncertainties, while the initial target volume PTV1 is to account for both position uncertainties and possible clonogen spread. The position uncertainties and the way to account for them have been widely discussed in the literature.³⁷⁻⁴¹ Following the ideas described in the article of Stavrev et al.³⁷ one can define a reduced cell density - a notion combining the initial cell density with the position uncertainties. We presume the initial cell density $H(\vec{r})$ constant over the GTV and the position uncertainties being described by a 3D normal distribution $G(\vec{r})$. Here H is the Heviside step function being 1 in the GTV and 0 outside. Then the relative reduced cell density is given as:

$$[9] \rho(\vec{r}) = \int_{R^3} G(\vec{r}) H(\vec{r} - \vec{\delta}) d^3\vec{\delta}$$

$$[10] T C P = e^{-\int_V \rho(\vec{r}) e^{-\alpha D(\vec{r})} d^3\vec{\delta}} = e^{-N_0 \sum \rho_{ijk} e^{-\alpha D_{ijk}}}$$

The parameters α, N_0 could be calculated directly from γ_{50}, D_{50} .²⁵ The possible clonogen spread may be modelled in a similar way. One can presume that a clonogen could leave its position and relocate at another one with a given probability. If the probability is presumed normal, it could be shown that Eq. [9] describes the process of migration as well. Hence, both processes could be described as convolutions of GTV with normal distributions with different standard deviations, which is equivalent to one convolution but the variance of the normal distribution is the sum of the first ones.

The clinical practice guidelines in our institution determine the PTV2 as GTV with 5 mm margin and PTV1 as GTV with 15 mm margin. Hence, having in mind the normality (the 99 % of the possible values of the stochastic variable lay in +3SD interval) of the position uncertainties and clonogen spread, we deduce that the first process is described with normal distribution with SD of ~1.6mm and the second one SD=3.2mm. Figure 2

demonstrates the GTV (the solid body) and the calculated reduced cell density, for the case under consideration.

Results

Figure 1 demonstrates isodose distributions for the 2-phased, SIB44 and SIB55 plans in the axial plane containing the treatment isocenter. Figure 3 illustrates the DVHs for the GTV, PTV1, bladder and rectum, as obtained for the 2-phased (solid line), SIB44

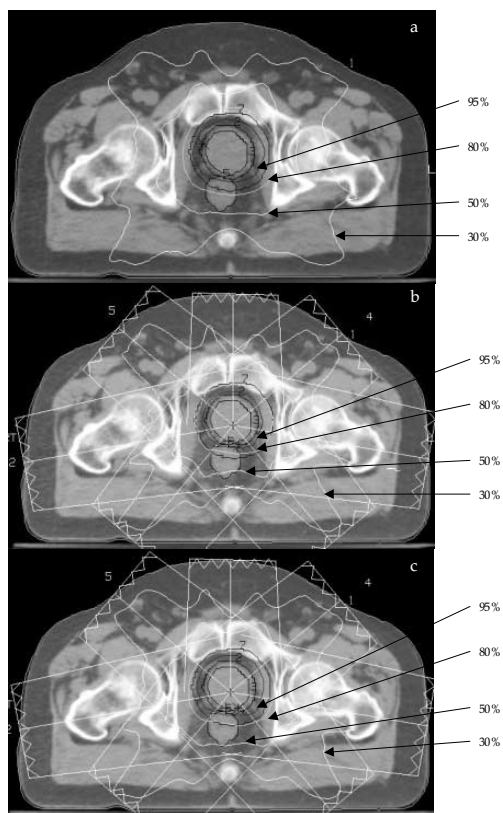


Figure 1. Set-up for 7-beam prostate treatment technique and central slice isodoses for (a) two-phase strategy, (b) - SIB 44, (c) - SIB 55. The PTV1 is denoted as 7, PTV2 - 2, GTV - 3, rectum - 5. The bladder is not seen on this slice. The 95 % isodose line lies between the PTV2 and PTV1 contours. The isodose distributions are normalized to 100 % at the treatment isocenter.

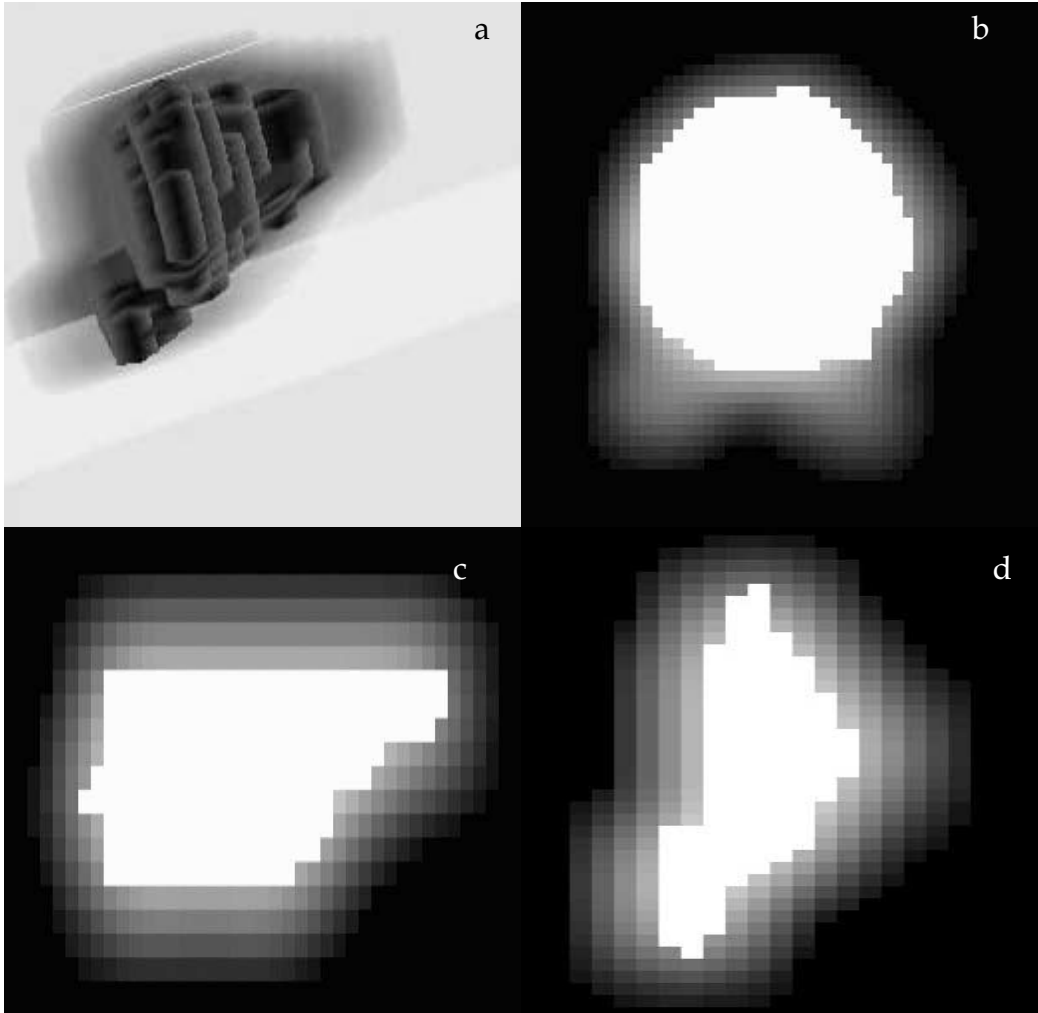


Figure 2. Illustration of the reduced cell density, accounting for the clonogen spread and position uncertainties Eq. [8]. The solid body represents the GTV surface on Figure (a), the reduced cell density »hallo« is shown for two perpendicular planes. On Figures (b), (c) and (d) cross-sections in three perpendicular planes (axial 2a, coronal 2b, sagittal 2c) with the GTV (the white object) and the reduced cell density are shown.

(dotted line) and SIB55 (dashed line) strategies. Both SIB strategies resulted in better sparing of the critical organs while satisfying the prescriptions with respect to the target volumes.

2-phased strategy

For the 2-phased strategy we have calculated the NTCPs for bladder and rectum using Eq.

[2], [5], [6] and have obtained the following values $NTCP_{\text{bladder}} = 5.2\%$ and $NTCP_{\text{rectum}} = 45\%$. The last represent the Lyman model $NTCP$ estimates. An estimate of bladder $NTCP$ was also obtained based on the CV model yielding the value of 8.25%. The TCP - Eq. [4] - based on the GTV BED distribution for the cases of $\alpha/\beta = 2$ and 10 Gy respectively is 93.1% and 84.2%. If the possible clono-

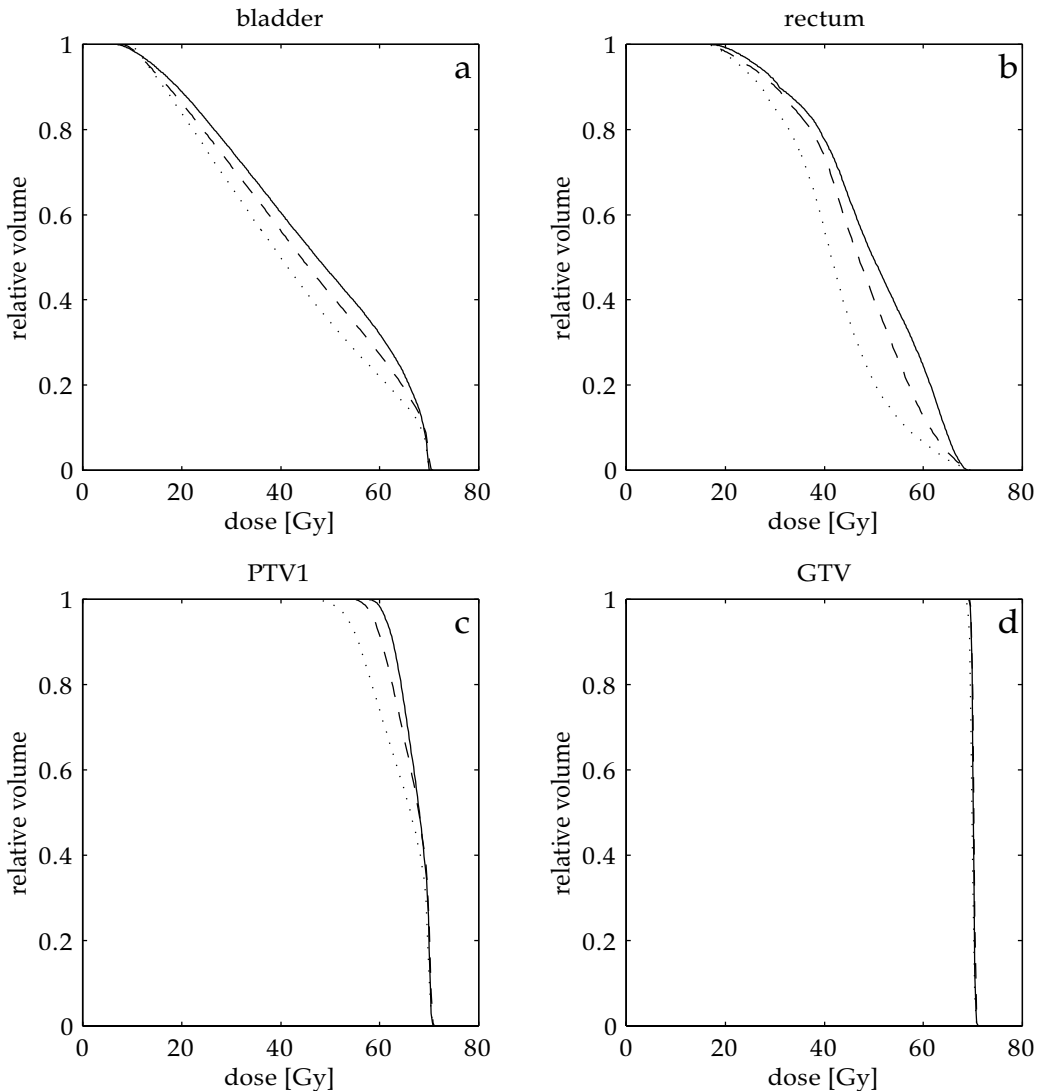


Figure 3. DVHs for the three different treatments and different structures: (a) bladder, (b) rectum, (c) PTV1, (d) GTV. The two-phase approach (solid line) prescribes 44 Gy to the first phase volume and additional 26 Gy to the boost one. The actual delivered minimal dose to the first phase volume was 55 Gy. These prompted us to investigate two SIB IMRT plans delivering minimal doses of 44 Gy (dotted line) and 55 Gy (dashed line) to the first phase volume respectively.

gen spread and the position uncertainties are taken into account using Eq. [9] and [10] one gets $TCP_{\alpha/\beta = 2} = 86\%$ and $TCP_{\alpha/\beta = 10} = 74.4\%$. The *TCP* and *NTCP* values for the 2-phased strategy are shown as lines parallel to the x-axes on Figures 4 a, b, c and d.

SIB strategy

The *NTCPs* for bladder and rectum, calculated again on the basis of Eq. [2], [5], [6], for SIB44 and SIB55 correspondingly, as a function of number of fractions are presented on

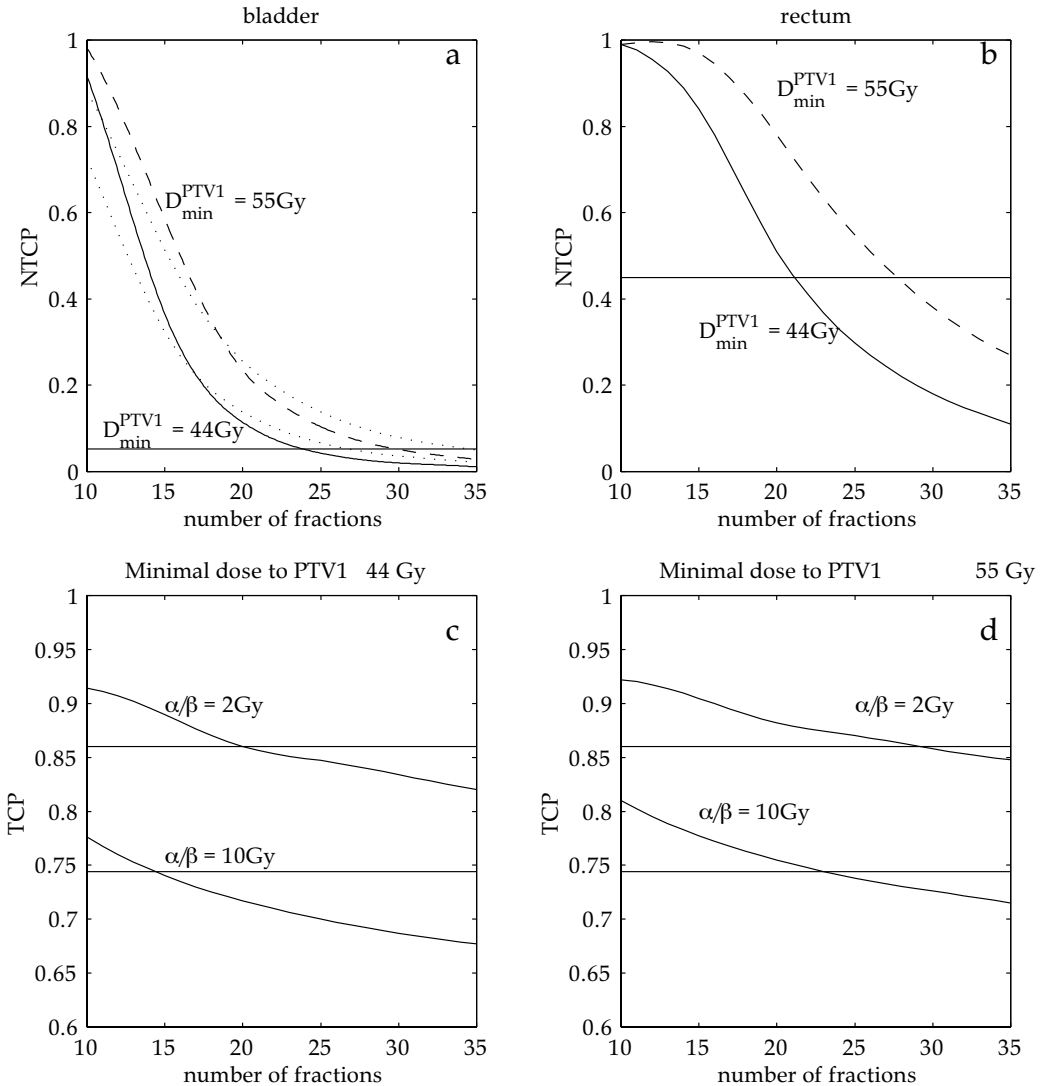


Figure 4. Figures (a) and (b) show the influence of the fractionation on the bladder and rectum NTCPs for the SIB treatment strategies. The horizontal line represents the NTCP for the two-phase treatment. Figures (c) and (d) demonstrate the dependence of the TCP, accounted for clonogen spreads and marginal uncertainties, on the number of fractions for the two different SIB treatment plans. Again the horizontal line represents the TCP for the two-phase treatment. The effect of a possible smaller α/β ratio (2 vs. 10 Gy) is demonstrated. Note the drop in the TCP for SIB55 fraction treatment compared to the two-phased method. Considering the SIB55, reducing the number of fractions to 25 ($\alpha/\beta = 10$ Gy) or 30 ($\alpha/\beta = 2$ Gy) in order to achieve the two-phase-equivalent-TCP will or will not reduce the bladder and rectum NTCPs below their values for the two-phase treatment (Figures 4a and 4b).

Figures 4a and 4b. Similarly the TCP, accounting for the clonogen spread and position uncertainties, as a function of number of fractions, for SIB44 is shown on Figure 4c and

for SIB55 on Figure 4d. The both different curves on those plots correspond to the two different α/β ratios.

In the case when the position uncertainties

and clonogen spread are disregarded the TCP change with the number of fractions become negligibly small $\sim 1.5\%$ / 10 fractions.

Discussion and conclusions

First it should be said, that the TCP and NTCP values and relationships calculated here must be regarded more as relative numbers illuminating the interrelation of the dose-volume effects and fractionation on one hand and the biological outcomes on the other.

It is clear from the DVHs shown on Figures 3a and 3b that the SIB strategy results in smaller doses delivered to the organs at risk. The dose delivered to GTV is equally uniform for the 2-phase and SIB strategy. Hence, from a point of view concerning the physical dose delivery the SIB strategy results in superior dose distributions. On the other hand while the 2-phase strategy is strictly tied to a given fractionation scheme, these is not true for the SIB one. Because of the difference in the dose distributions in PTV1 the impact on the possible clonogen spread and position uncertainty would be different. As it is seen from Figures 4c and 4d there is considerable drop (up to 7%) in the TCP when the SIB strategy is applied in the same number of fractions as the 2-phased one - 35 in our case. The comparison between Figures 4c and 4d illustrates, as expected, that this difference is smaller for SIB55 compared to SIB44, and also for the $\alpha/\beta = 2$ Gy over $\alpha/\beta = 10$ Gy. Figures 4c and 4d also demonstrate the magnitude of the α/β ratio impact over the TCP. The difference between the TCPs calculated for 2 Gy and 10 Gy α/β ratios is about 15% for SIB44 and 11% for SIB55, almost independent of the number of fractions. The same goes for the 2-phased strategy. Thus the effect of the different α/β ratios is very significant and although more detailed studies may end up with different, than the one used here, model param-

eters, this would only shift up or down the TCP values but the impact on the TCP difference will be negligible. Hence, this result (Figures 4c and 4d) may be used as a hint of support for Brener's statement^{12,13} in the light of the findings of Logue et al.¹⁶ for relatively high local control.

Let us presume all the model parameters correctly estimated and consider the implication of the results shown on Figure 3. For the case $\alpha/\beta = 10$ Gy and minimum of 44 Gy to PTV1, Figure 4c shows that if the SIB IMRT dose is delivered in 15 fractions it will result in the same TCP as the conventional 2-phase strategy. For the normal tissue, we get 24 and 21 fractions for bladder and rectum respectively. Hence in this case, regardless of the fractionation regime, either the TCP would be lower than the 2-phased strategy TCP, or the NTCP would be higher than the 2-phased strategy NTCP. This is quite natural, because the minimum dose to PTV1 in the conventional therapy was 55 Gy, not 44 Gy. When the optimization is done with the requirement - 55 Gy to PTV1, then one gets 24, 30 and 27 fractions for the tumour, bladder and rectum, respectively in order to achieve the same effect, as in the 2-phase strategy. In the case $\alpha/\beta = 2$ Gy the situation is much better! The SIB44 plan leads to equivalent TCP at 21 fractions, and SIB55 at 29 fractions. In both cases, a 23 (or 29 for SIB55) fraction regime would lead to almost similar TCP for the tumour and NTCP for the bladder, while the NTCP for rectum will diminish.

Now we should return to the question which most probably the reader has already asked himself - *Why the value of NTCP for the rectum is so high?* The answer to this question is simple - the parameter values of the Lymans model^{8,35} were calculated based on the nominal dose and in this case the usage of BED is improper. The use of Eq. [3] is equally incorrect. The NTCP values for bladder and rectum calculated using the nominal dose are .02% and 4 % correspondingly - these num-

bers are quite acceptable as expected NTCPs. If calculated on the bases of Eq. [3] the NTCP values are almost negligible. On the other hand the fractionation effect could be accounted for only if BED (or Eq. [3]) is used with Lyman's model. For the CV model the use of BED is equivalent of directly applying the LQ model of cell damage, when assessing the P_{FSU}^{25} a feature intrinsic to this model.

Figure 4a - NTCP for bladder as a function of number of fractions - illustrates eloquently the difference between the Lyman and the CV model. The parameters for both models were estimated from the »Emami data«, but for the small probabilities (high number of fractions) $NTCP_{CV}$ is slightly higher than $NTCP_{Lyman}$ and vice-versa for higher probabilities (smaller number of fractions).

The potential of inverse planning to design tight conformal distributions is fully revealed when all relevant organs and targets along with the corresponding dosimetric constraints (in terms of total doses) are considered in a single optimization process. However, the delivery of such plans may generally require modifications of existing fractionation regimes in order to assure similar outcomes.

For the case of SIB prostate IMRT, accounting for position uncertainties and possible clonogen spreads, we have estimated the radiobiological effect of various fractionation schemes using existing TCP/NTCP models. Although, some of the model parameters are not quite reliable, the models illuminate the major TCP/NTCP interrelations as a function of the number of fractions. It has been demonstrated that the optimized SIB superior dose distributions may not always lead to better tumour control and tissue sparing and therefore careful selection of the fractionation regime is required.

References

1. Mohan R, Wu Q, Manning M, Schmidt-Ullrich R. Radiobiological considerations in the design of fractionation strategies for intensity-modulated radiation therapy of head and neck cancers. *Int J Radiat Oncol Biol Phys* 2000; **46**: 619-30.
2. Wu Q, Manning M, Schmidt-Ullrich R, Mohan R. The potential for sparing of parotids and escalation of biologically effective dose with intensity-modulated radiation treatments of head and neck cancers: a treatment design study. *Int J Radiat Oncol Biol Phys* 2000; **46**: 195-205.
3. Lebesque JV, Keus RB. The simultaneous boost technique: the concept of relative normalized total dose. *Radiother Oncol* 1991; **22**: 45-55.
4. Knee R, Fields RS, Peters LJ. Concomitant boost radiotherapy for advanced squamous cell carcinoma of the head and neck. *Radiother Oncol* 1985; **4**: 1-7.
5. Heukelom S, Lanson JH, Mijnheer BJ. Quality assurance of the simultaneous boost technique for prostatic cancer: dosimetric aspects. *Radiother Oncol* 1994; **30**: 74-82.
6. Essers M, Lanson JH, Mijnheer BJ. In vivo dosimetry during conformal therapy of prostatic cancer. *Radiother Oncol* 1993; **29**: 271-9.
7. Stavrev PV, Hristov DH, Seuntjens JP. On the consistent use of organ definitions and radiobiological models for the evaluation of complication probabilities of tubular organs. *Int J Radiat Oncol Biol Phys* 2002; **52**: 1150-2.
8. Burman C, Kutcher GJ, Emami B, Goitein M. Fitting of normal tissue tolerance data to an analytic function. *Int J Radiat Oncol Biol Phys* 1991; **21**: 123-35.
9. Okunieff P, Morgan D, Niemierko A, Suit HD. Radiation dose-response of human tumors. *Int J Radiat Oncol Biol Phys* 1995; **32**: 1227-37.
10. Stavrev P, Stavreva N, Niemierko A, Goitein M. The Application of biological models to clinical data. *Phys Medica* 2001; **17**: 71-82.
11. Dale E, Hellebust TP, Skjonsberg A, Hogberg T, Olsen DR. Modeling normal tissue complication probability from repetitive computed tomography scans during fractionated high-dose-rate brachytherapy and external beam radiotherapy of the uterine cervix. *Int J Radiat Oncol Biol Phys* 2000; **47**: 963-71.
12. Brenner DJ. Toward optimal external-beam frac-

- tionation for prostate cancer. *Int J Radiat Oncol Biol Phys* 2000; **48**: 315-6.
13. Brenner DJ, Hall EJ. Fractionation and protraction for radiotherapy of prostate carcinoma. *Int J Radiat Oncol Biol Phys* 1999; **43**: 1095-101.
 14. King CR, Mayo CS. Is the prostate alpha/beta ratio of 1.5 from Brenner & Hall a modeling artifact. *Int J Radiat Oncol Biol Phys* 2000; **47**: 536-9.
 15. Brenner DJ, Hall EJ. In response to Drs. King and Mayo: Low alpha/beta values for prostate appear to be independent of modeling details. *Int J Radiat Oncol Biol Phys* 2000; **47**: 538-9.
 16. Logue JP, Cowan RA, Hendry JH. Hypofractionation for prostate cancer. *Int J Radiat Oncol Biol Phys* 2001; **49**: 1522-3.
 17. Brenner DJ. Hypofractionation for prostate cancer - In response. *Int J Radiat Oncol Biol Phys* 2001; **49**: 1522-3.
 18. Dale E, Olsen DR, Fossa SD. Normal tissue complication probabilities correlated with late effects in the rectum after prostate conformal radiotherapy. *Int J Radiat Oncol Biol Phys* 1999; **43**: 385-91.
 19. Lyman JT. Complication probability as assessed from dose-volume histograms. *Radiat Res* 1985; **8(Suppl 1)**: S13-9.
 20. Niemierko A, Goitein M. Modeling of normal tissue response to radiation: the critical volume model. *Int J Radiat Oncol Biol Phys* 1993; **25**: 135-45.
 21. Jackson A, Kutcher GJ, Yorke ED. Probability of radiation-induced complications for normal tissues with parallel architecture subject to non-uniform irradiation. *Med Phys* 1993; **20**: 613-25.
 22. Yorke ED, Kutcher GJ, Jackson A, Ling CC. Probability of radiation-induced complications in normal tissues with parallel architecture under conditions of uniform whole or partial organ irradiation. *Radiother Oncol* 1993; **26**: 226-37.
 23. Jackson A, Ten Haken RK, Robertson JM, Kessler ML, Kutcher GJ, Lawrence TS. Analysis of clinical complication data for radiation hepatitis using a parallel architecture model. *Int J Radiat Oncol Biol Phys* 1995; **31**: 883-91.
 24. Niemierko A. Present and future of the clinical use of radiobiological models in radiation therapy treatment planning. *Phys Medica* 1997; **13**: 34-8.
 25. Stavrev P, Stavreva N, Niemierko A, Goitein M. Generalization of a model of tissue response to radiation based on the idea of functional subunits and binomial statistics. *Phys Med Biol* 2001; **46**: 1501-18.
 26. Niemierko A, Goitein M. Calculation of normal tissue complication probability and dose-volume histogram reduction schemes for tissues with a critical element architecture. *Radiother Oncol* 1991; **20**: 166-76.
 27. Lyman JT, Wolbarst AB. Optimization of radiation therapy, III: a method of assessing complication probabilities from dose-volume histograms. *Int J Radiat Oncol Biol Phys* 1987; **13**: 103-9.
 28. Kutcher GJ, Burman C, Brewster L, Goitein M, Mohan R. Histogram reduction method for calculating complication probabilities for three-dimensional treatment planning evaluations. *Int J Radiat Oncol Biol Phys* 1991; **21**: 137-46.
 29. Kutcher GJ, Burman C. Calculation of complication probability factors for non-uniform normal tissue irradiation: the effective volume method. *Int J Radiat Oncol Biol Phys* 1989; **16**: 1623-30.
 30. Niemierko A. A generalized concept of Equivalent Uniform Dose. [Abstract]. 41th AAPM Annual Meeting, Nashville, 24-29 July. *Med Phys* 1999; **26**: 1100.
 31. Lebesque JV, Bruce AM, Kroes AP, Touw A, Shouman RT, van Herk M. Variation in volumes, dose-volume histograms, and estimated normal tissue complication probabilities of rectum and bladder during conformal radiotherapy of T3 prostate cancer. *Int J Radiat Oncol Biol Phys* 1995; **33**: 1109-19.
 32. Ting JY, Wu X, Fiedler JA, Yang C, Watzich ML, Markoe A. Dose-volume histograms for bladder and rectum. *Int J Radiat Oncol Biol Phys* 1997; **38**: 1105-11.
 33. Boersma LJ, van den Brink M, Bruce AM, Shouman T, Gras L, te Velde A, et al. Estimation of the incidence of late bladder and rectum complications after high-dose (70-78 Gy) conformal radiotherapy for prostate cancer, using dose-volume histograms. *Int J Radiat Oncol Biol Phys* 1998; **41**: 83-92.
 34. Jackson A, Skwarchuk MW, Zelefsky MJ, Cowen DM, Venkatraman ES, Levegrun S, et al. Late rectal bleeding after conformal radiotherapy of prostate cancer. II. Volume effects and dose-volume histograms. *Int J Radiat Oncol Biol Phys* 2001; **49**: 685-98.
 35. Emami B, Lyman J, Brown A, Coia L, Goitein M, Munzenrider JE, et al. Tolerance of normal tissue to therapeutic irradiation. *Int J Radiat Oncol Biol Phys* 1991; **21**: 109-22.
 36. Hartford AC, Niemierko A, Adams JA, Urie MM, Shipley WU. Conformal irradiation of the

- prostate: estimating long-term rectal bleeding risk using dose-volume histograms. *Int J Radiat Oncol Biol Phys* 1996; **36**: 721-30.
37. Stavrev PV, Stavreva NA, Round WH. A new method for optimum dose distribution determination taking tumour mobility into account. *Phys Med Biol* 1996; **41**: 1679-89.
 38. Lind BK, Kallman P, Sundelin B, Brahme A. Optimal radiation beam profiles considering uncertainties in beam patient alignment. *Acta Oncol* 1993; **32**: 331-42.
 39. Lof J, Lind BK, Brahme A. An adaptive control algorithm for optimization of intensity modulated radiotherapy considering uncertainties in beam profiles, patient set-up and internal organ motion. *Phys Med Biol* 1998; **43**: 1605-28.
 40. Mageras GS, Kutcher GJ, Leibel SA, Zelefsky MJ, Melian E, Mohan R, et al. A method of incorporating organ motion uncertainties into three-dimensional conformal treatment plans. *Int J Radiat Oncol Biol Phys* 1996; **35**: 333-42.
 41. Rudat V, Schraube P, Oetzel D, Zierhut D, Flentje M, Wannemacher M. Combined error of patient positioning variability and prostate motion uncertainty in 3D conformal radiotherapy of localized prostate cancer. *Int J Radiat Oncol Biol Phys* 1996; **35**: 1027-34.